



# Homogeneous one-pot synthesis of ZnCMC nanoparticles via intermediate-state autocatalyzed carboxymethylation of cellulose

Heloise O. M. A. Moura<sup>1,2\*</sup>, Jordanna L. B. Costa<sup>1</sup>, Eduarda S. Pereira<sup>1</sup>, Aisha V. S. Pereira<sup>1</sup>, Daniella N. R. do Nascimento<sup>2</sup>, Gustavo Oliveira de Paula<sup>1</sup>, Késia K. de O. S. Silva<sup>2</sup>, Daniel B. Plata<sup>3</sup>, Enrique Rodríguez-Castellón<sup>3</sup>, Luciene S. de Carvalho<sup>1</sup>

<sup>1</sup>Energetic Technologies Laboratory – LABTEN, Institute of Chemistry, Federal University of Rio Grande do Norte, 59078-900, Natal, Brazil.

<sup>2</sup>Post-graduate Program in Textile Engineering – PPGET, Technology Center, Federal University of Rio Grande do Norte, 59078-900, Natal, Brazil.

<sup>3</sup>Department of Inorganic Chemistry, Crystallography and Mineralogy, College of Sciences, University of Málaga, 29071 Málaga, Spain.

\*helo.medeiros@outlook.com

## Resumo/Abstract

RESUMO - Esta pesquisa explora a carboximetilação ultrarrápida em meio homogêneo da celulose utilizando hidrato salino de cloreto de zinco (ZnCl<sub>2</sub>·3H<sub>2</sub>O) como solvente verde, sem a necessidade de ativação prévia com NaOH. A carboxilação inicia-se após apenas 10 minutos de reação, e os produtos são recuperados com solventes orgânicos "verdes" após tempos de reação variando de 30 minutos a 5 horas. O método resulta em um novo polímero de biocoordenação nanométrico (10–36 nm), solúvel em água, denominado nano ZnCMC, formado pela complexação de cátions de zinco com os grupos carboxilato da CMC. Análises espectroscópicas e microscópicas confirmam sua composição e morfologia. As nanopartículas de ZnCMC auto-organizam-se em supracristais cúbicos por meio de interações coulômbicas entre os clusters carregados [Zn<sub>4</sub>O(RCO<sub>2</sub>)<sub>6</sub>]<sup>2+</sup> e ânions cloreto provenientes do excesso de NaCl, imitando a unidade de construção secundária (SBU) e a microestrutura do MOF-5. Produzido a partir de fontes renováveis e utilizando reagentes não tóxicos e reutilizáveis, este material oferece aplicações promissoras em nanotecnologia, catálise, sensores e fotônica, alinhando-se aos princípios da Química Verde.

Palavras-chave: Dissolução da celulose; Conversão homogênea; Polímero de coordenação; Nanomaterial; Autocatálise.

ABSTRACT - This research explores the ultrarapid, homogeneous carboxymethylation of cellulose using zinc chloride molten salt hydrate ( $ZnCl_2 \cdot 3H_2O$ ) as a green solvent, without prior NaOH activation. Carboxylation begins after just 10 minutes of reaction, with products recovered using eco-friendly organic solvents after varying reaction times (30 min to 5 h). The method yields a novel, water-soluble, nanometric (10–36 nm) biocoordination polymer, nano ZnCMC, formed by the complexation of zinc cations with the carboxylate groups of CMC. Spectroscopic and microscopic analyses confirm its composition and morphology. ZnCMC nanoparticles self-assemble into cubic supracrystals via coulombic interactions between charged [ $Zn_4O(RCO_2)_6$ ]<sup>2+</sup> clusters and chloride anions from excess NaCl, mimicking the secondary building unit (SBU) and microstructure of MOF-5. Produced from renewable sources using non-toxic, reusable reagents, this material offers promising applications in nanotechnology, catalysis, sensing, and photonics, aligning with Green Chemistry principles.

Keywords: Cellulose dissolution; Homogeneous conversion; Coordination polymer; Nanomaterial; Autocatalysis.

## Introduction

Cellulose is a polysaccharide consisting of glucose monomers linked by  $\beta$ 1,4-glycosidic bonds and is the most widely explored lignocellulosic fraction in biorefineries, with extremely promising studies for application in high-tech materials and nanomaterials, among other industries (1). Sodium carboxymethylcellulose (CMCNa) is one of the most commercially relevant cellulose derivatives, whose composites stand out in a series of studies in the areas of batteries, biosensors, controlled release of drugs and fertilizers, adsorbents and catalysts (2-5) due to its water-solubility, low cost, biocompatibility, and biodegradability

characteristics, in addition to its ability to form complexes due to its multiple carboxylate groups that replace the native hydroxyl groups of cellulose.

These properties make CMC a promising carbohydrate derived macromolecule for studies in bio-based coordination polymers (CPs) and metal organic frameworks (MOFs), which is an emerging field with few researches (6); however, most methods of synthesis are very time-consuming, employ toxic organic solvents and fossil carbon-based rigid aromatic ligands (7).

A bottleneck for its application as bio-ligand in coordination chemistry is the heterogeneous nature of the



derivatization of cellulose to CMC. Since cellulose is a crystalline polysaccharide due to the large amount of hydrogen bonds between the hydroxyls of its chains, dissolving cellulose is a challenge for both research and industrial applications. In this research, the molten salt hydrate ZnCl<sub>2</sub>.3H<sub>2</sub>O (zinc chloride trihydrate) was selected as solvent for cellulose and reaction medium, due to its promising efficiency. Its ions intercalate the cellulose fibers, breaking the hydrogen bonds through the complexation of the Zn<sup>2+</sup> cation by the hydroxyls in its chains and allowing the ultra-rapid dissolution (within 25 min) of approximately 100% of the cellulosic fibers under mild conditions (8,9). It is also considered a green solvent, since it has low toxicity, high biocompatibility and can be regenerated and reused in multiple cycles of cellulose dissolution processes.

This work reports an innovative study in the one-pot carboxymethylation of cellulose in homogenous media, using  $ZnCl_2.3H_2O$  as solvent under mild conditions, in an autocatalysis process without previous activation with NaOH. A set of characterization techniques were used for assessing its structure and composition, and the reaction mechanism was proposed with base in the literature.

# Experimental

Materials

Microcrystalline cellulose (Avicel® PH-101) and anhydrous  $ZnCl_2$  ( $\geq 98\%$ ) were obtained from Sigma-Aldrich. Monochloroacetic acid, 2-propanol, and commercial NaCMC (P.A.) were supplied by Synth. Diethyl ether and anhydrous NaCl ( $\geq 99\%$ ) were purchased from Vetec and Anidrol, respectively.

#### Synthesis of ZnCMC nanoparticles

Anhydrous ZnCl<sub>2</sub> was mixed with distilled water to form ZnCl<sub>2</sub>·3H<sub>2</sub>O, which is a liquid salt hydrate at NTP (molten salt), and microcrystalline cellulose (2% w/w) was dissolved in it at 90 °C, yielding a clear, viscous solution called ZnCel. The mixture was then cooled to 75 °C, and NaCl was added under stirring up to saturation.

Carboxymethylation was initiated by adding monochloroacetic acid (MCA:AGU = 10:1), with reaction times ranging from 10 min to 5 h. The medium remained homogeneous throughout. Products were recovered using a 2:1 (v/v) 2-propanol:diethyl ether mixture, washed, centrifuged, and dried at 50 °C. Samples were labeled according to reaction time (e.g., Z0.5 had a reaction time of 0.5 h).

#### Characterizations

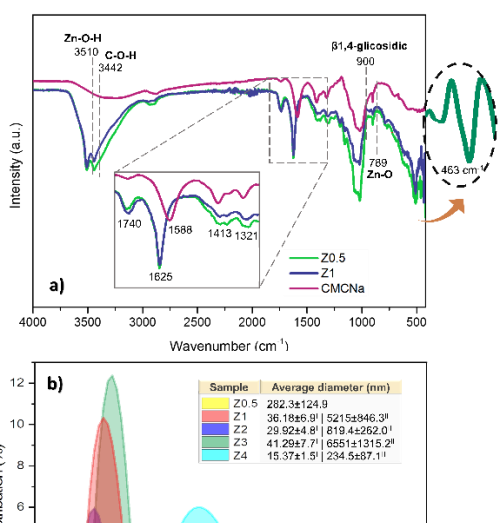
Fourier transform infrared (FTIR) spectra were acquired using a Shimadzu IRAffinity-1 with ATR (32 scans, 4 cm<sup>-1</sup> resolution, 400–4000 cm<sup>-1</sup>). X-ray photoelectron spectroscopy (XPS) was carried out in a PHI 5700 system with AlK $\alpha$  radiation. Dynamic light scattering (DLS) was



performed with a Litesizer 500, using a 658 nm laser, immediately after suspending ZnCMC nanoparticles in diethyl ether. Morphological analysis included SEM (TESCAN MIRA, 10 kV, gold-coated samples) and high-resolution TEM/STEM (Talos<sup>TM</sup> F200X G2 at 200 kV, HAADF detector) microscopies, along with energy-dispersive X-ray spectroscopy (EDS) mapping using four in-column SDD Super-X detectors.

#### Results and Discussion

Characteristic absorption bands of CMC are observed at 1740 cm<sup>-1</sup>, 1588 cm<sup>-1</sup>, and 1413 cm<sup>-1</sup> in the FTIR spectrum of commercial CMCNa (Figure 1a), corresponding to the symmetric stretching of C=O and the asymmetric and symmetric stretching of -COO<sup>-</sup> in the deprotonated form, respectively (10,11). A similar profile is seen in ZnCMC nanoparticles, with bands at 1740 cm<sup>-1</sup>, 1625 cm<sup>-1</sup>, and 1409 cm<sup>-1</sup>. The shift of the asymmetric -COO<sup>-</sup> band to higher wavenumber aligns with values reported for CMCNa obtained via standard synthesis (11) and may also reflect Zn<sup>2+</sup> coordination to carboxylate groups, which can cause a redshift (10,12).



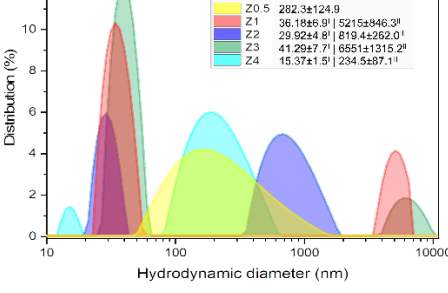


**Figure 1.** a) FTIR spectra for commercial CMCNa and nano ZnCMC samples produced in 30 min and 1 h (Z0.5 and Z1); b) hydrodynamic diameter (HD) distribution curves for nano ZnCMC samples.

The O-H stretching region (3000–3650 cm<sup>-1</sup>) differs significantly between spectra: commercial CMC shows a broad, weak band due to adsorbed water and hydrogenbonded hydroxyl groups, while nano ZnCMC exhibits two



sharp, intense peaks at 3510 cm<sup>-1</sup> and 3442 cm<sup>-1</sup>, assigned to free Zn–O–H and C–O–H stretches, respectively (12). This split does not appear in all samples, suggesting the Zn–O–H band may arise from Zn<sup>2+</sup> coordination with water.

Additional absorption bands at 789 cm<sup>-1</sup>, 509 cm<sup>-1</sup>, and 435 cm<sup>-1</sup> correspond to Zn–O stretching, while features at 463 cm<sup>-1</sup> and 526 cm<sup>-1</sup> suggest the formation of tetrahedral Zn<sub>4</sub>O clusters coordinated to CMC carboxylate groups, similar to networks found in Zn-based CPs and MOFs (13). The presence of C–O stretching bands between 1150 and 1000 cm<sup>-1</sup> and the β-1,4-glycosidic vibration at 900 cm<sup>-1</sup> (11) confirm the preservation of the cellulose backbone. The FTIR spectra of nano ZnCMC produced at longer reaction times also showed consistent band positions, with variations in relative intensities.

The results of hydrodynamic diameter (HD) analyzed by DLS for nano ZnCMC precipitated at different reaction times are shown in Figure 1b. Except for the sample Z0.5, all the samples presented a bimodal size distribution representing small size nanoparticles (average HD < 42 nm) and a contribution of micro sized nanoparticle aggregates, which occurs due to the high interparticle interaction. Although the high aggregation, the polydispersity index (PDI) of all samples was below 0.3 (except for Z2, PDI = 0.43), which is acceptable for pharmacologic applications, for example, and indicates a homogenous population in the size of the particles produced (14). XPS analysis revealed characteristic peaks for C 1s, O 1s, Zn 2p, Na 1s, and Cl 2p photoemission electrons (Figure 2a).

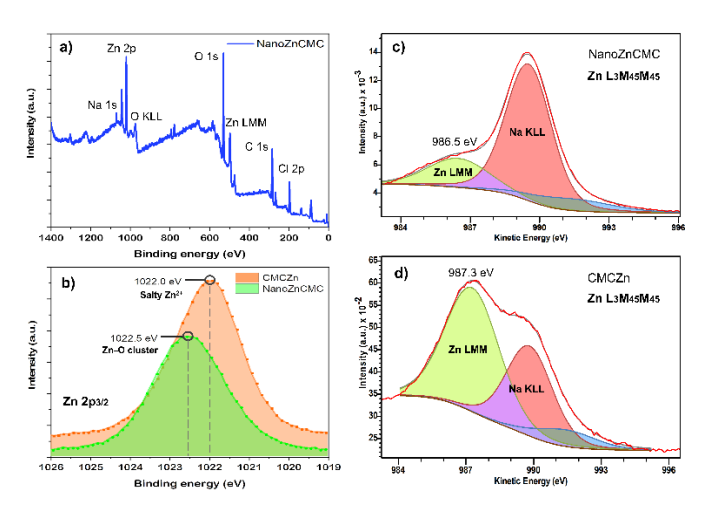


**Figure 2.** a) Survey XPS spectrum of nano ZnCMC, b) Zn 2p3/2 spectrum, and Zn LMM peak deconvolution for c) nano ZnCMC and d) CMCZn samples.

The high-resolution O 1s spectrum of nano ZnCMC showed four components at 533.1 eV (C–OH), 532.4 eV (C=O), 531.6 eV (–COO<sup>-</sup>), and 530.8 eV (Zn–O lattice) (15). The C 1s spectrum displayed peaks at 288.1 eV (O=C–O), 286.6 eV (C=O), 285.5 eV (–CH<sub>3</sub> from carboxymethyl),



and 284.5 eV (C–C/C=C/adventitious carbon), confirming successful cellulose carboxymethylation and Zn<sup>2+</sup> complexation (16,17).

Commercial CMCNa precipitated from ZnCl<sub>2</sub>.3H<sub>2</sub>O hydrate (CMCZn) was analyzed for comparison. Symmetrical Zn 2p<sub>3</sub>/<sub>2</sub> peaks for nano ZnCMC (1022.5 eV) and CMCZn (1022.0 eV) (Figure 2b) indicate Zn<sup>2+</sup> species, with the shift to higher BE in nano ZnCMC attributed to Zn(II) coordination in a more electronegative environment (13,18). Zn LMM Auger spectra (Figures 2c and 2d) confirmed Zn<sup>2+</sup> through modified Auger parameters:  $\alpha$ ' = 2009.0 eV (nano ZnCMC) and  $\alpha$ ' = 2009.3 eV (CMCZn), with kinetic energies of 986.5 eV and 987.3 eV, respectively. An additional signal around 990 eV corresponds to Na KLL Auger electrons, more intense in nano ZnCMC due to excess NaCl used in synthesis.

SEM analysis revealed the initial formation of cubic microcrystals after 1 h of synthesis (Figure 3). From 2 h of synthesis onward (Z2 and Z3), the formation of well-defined cubic crystals with variable sizes was observed, consistent with reports for analogous materials such as MOF-5 and Zn–BCPA (18,19). The cubes, with edge lengths between 0.2 and 1.7  $\mu$ m (from TEM, STEM, and SEM), correspond to surface areas of 8–17  $\mu$ m², though larger particles were also identified (Figure 3d). High-magnification images of Z3 (Figures 3e–f), along with HAADF-STEM and HRTEM (Figure 4), confirmed that these cubes are aggregates of ZnCMC nanoparticles.

FT-treated edge images (Figure 4g) reveal a tendency toward superstructure organization. Elemental mapping by EDS (Figure 4h) shows that carbon is the predominant element in nanoZnCMC, consistent with its metal-organic nature and with values reported for zinc-based CPs such as MOF-5. Among the samples, Z2 exhibited a higher surface carbon content (~20%) and reduced Na and Cl levels, suggesting greater exposure of the CMC backbone. Despite its utility, EDS has limited accuracy for light elements (Z < 11), and excess NaCl may hinder the detection of other atoms due to surface deposition.

The formation of nano ZnCMC supracrystals likely results from electrostatic interactions involving Zn²+, Na+, and Cl⁻ ions, which act as "ionic glue" that binds nanoparticles into ordered cubic structures — analogous to reports on colloidal crystals in the literature (20,21). Zn²+ is complexed with carboxylate groups in Zn–O clusters, while Na+ and Cl⁻ remain as free ions interacting with charged nanoparticle surfaces, which may also explain their lower EDS signal intensity. With basis in these results, a mechanism is proposed to justify the efficiency of this homogeneous carboxymethylation medium (Figure 5) without previous NaOH activation, which is employed in the conventional heterogeneous method for the deprotonation of cellulose hydroxyls.



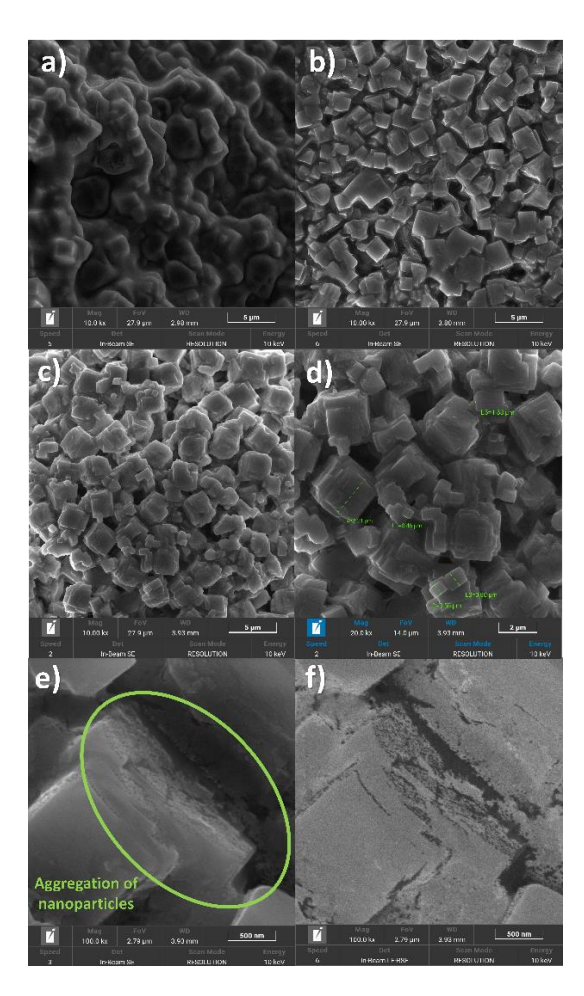


**Figure 3.** SEM micrographs for a) Z1, b) Z2 and c) Z3, respectively, and higher magnification images of Z3 at (d and e) 20.0 kx and f) 100.0 kx.

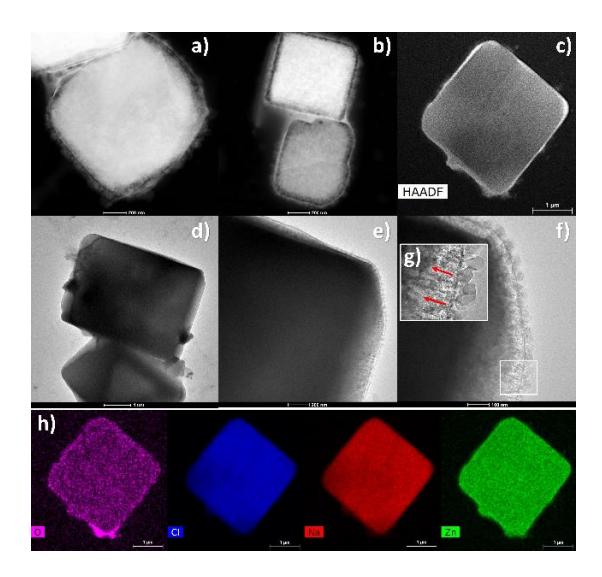


**Figure 4.** HAADF-STEM images for a) Z1, b) Z2 and c) Z3; HRTEM for Z3 with d) 1  $\mu$ m, e) 200 nm and f) 100 nm scale bar; g) FT-treated cutout and h) EDS elemental mapping of Z3.



According to Sen et al. (2016) (8), ZnCl<sub>2</sub>·3H<sub>2</sub>O behaves like an ionic liquid, existing as [Zn(OH<sub>2</sub>)<sub>6</sub>]<sup>2+</sup> and [ZnCl<sub>4</sub>]<sup>2-</sup> counterions. Their data show that the primary hydroxyl group of cellulose can replace a coordinated water molecule in [Zn(OH<sub>2</sub>)<sub>6</sub>]<sup>2+</sup>, forming part of the first coordination sphere, while secondary hydroxyls and [ZnCl<sub>4</sub>]<sup>2-</sup> interact via hydrogen bonding in the second coordination sphere. Based on these findings and previous studies on complex-mediated substitution (22)and Zn-carboxylate clusters coordination polymers (23), the carboxymethylation mechanism would involve substitution at the primary alcohol and potential formation of charged tetrahedral Zn-O clusters. Other hydroxyl substitutions are not excluded, and ongoing computational studies aim to clarify the conversion mechanism and the influence of NaCl and coordination environments in nanoZnCMC.

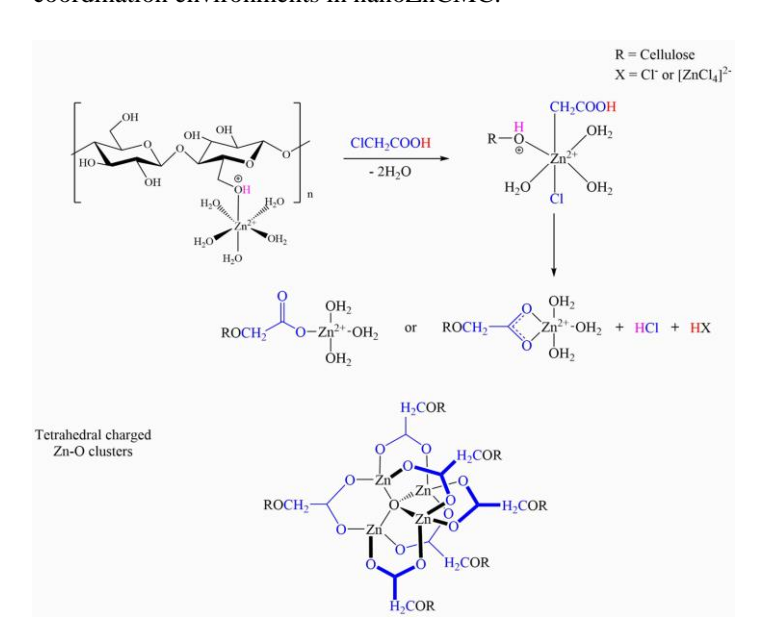


**Figure 5.** Proposed carboxymethylation reaction autocatalytic pathway and plausible Zn-O clusters for the nano ZnCMC CP.

# Conclusions

This study presents significant advances in homogeneous cellulose derivatization using ZnCl<sub>2</sub>·3H<sub>2</sub>O, highlighting the activation of substitution sites via zinc coordination and the complex's autocatalytic role during carboxymethylation. The developed method enables rapid, mild, and sustainable synthesis of water-soluble ZnCMC coordination polymer nanoparticles. As the first reported nanoscale cellulose-based bio-coordination polymer, nano ZnCMC exhibits unique properties, including nanoparticle self-assembly into cubic colloidal crystals driven by electrostatic interactions with excess NaCl. Its biodegradability, biocompatibility, nanoscale dimensions, and supracrystal-forming ability make it a promising candidate for applications in



nanotechnology reported for analogue materials, such as sensing, drug and fertilizer delivery, catalysis, and photonics.

# Acknowledgements

The authors acknowledge the support provided by the Post-Graduate Program in Chemistry (PPGQ/UFRN); the Analytical Center of the Institute of Chemistry (IQ/UFRN); the Molecular Sieves Laboratory (LABPEMOL/UFRN) and the University of Málaga for the analysis. Heloise O. M. A. Moura thanks to the Conselho Nacional Desenvolvimento Científico e Tecnológico – Brazil (CNPq) for the financial support (Finance Code 154372/2019-6); Enrique Rodríguez-Castellón and Daniel Ballesteros-Plata thank to the project PID2021-126235OB-C32 funded by MCIN/AEI/10.13039/501100011033/ and FEDER funds.

## References

- 1. Freire, C. S.; Vilela, C. Nanomaterials 2022, 12, 431.
- 2. Xu, L.; Meng, T.; Zheng, X.; Li, T.; Brozena, A. H.; Mao, Y.; Zhang, Q.; Clifford, B. C.; Rao, J.; Hu, L. *Adv. Funct. Mater.* **2023**, *33*, 2302098.
- 3. Nazarbek, U.; Nazarbekova, S.; Raiymbekov, Y.; Kambatyrov, M.; Abdurazova, P. *e-Polymers* **2023**, *23*, 20230013.
- 4. Kong, Q.; Zhang, H.; Wang, P.; Lan, Y.; Ma, W.; Shi, X. *Int. J. Biol. Macromol.* **2023**, 244, 125169.
- 5. Tan, Z.; Tan, J.; Yang, Z.; Sun, W.; Guo, A.; Wang, J.; Li, Y.; Lin, X. *Chemosphere* **2023**, *335*, 139129.
- 6. Wang, H. S.; Wang, Y. H.; Ding, Y. *Nanoscale Adv.* **2020**, 2, 3788–3797.
- Engel, E. R.; Scott, J. L. Green Chem. 2020, 22, 3693– 3715.
- Sen, S.; Losey, B. P.; Gordon, E. E.; Argyropoulos, D. S.; Martin, J. D. J. Phys. Chem. B 2016, 120, 1134–1141.
- 9. Chen, Y.; Yu, H. Y.; Li, Y. ACS Sustain. Chem. Eng. **2020**, 8, 18446–18454.
- 10. Ellerbrock, R. H.; Gerke, H. H. *J. Plant Nutr. Soil Sci.* **2021**, *184*, 388–397.
- 11. Mondal, M. I. H.; Yeasmin, M. S.; Rahman, M. S. *Int. J. Biol. Macromol.* **2015**, *79*, 144–150.
- 12. Wypych, F.; Arízaga, G. G. C.; da Costa Gardolinski, J. E. F. *J. Colloid Interface Sci.* **2005**, 283, 130–138.
- 13. Li, M.; Xu, Z.; Chen, Y.; Shen, G.; Wang, X.; Dai, B. *Nanomaterials* **2021**, *12*, 98.
- 14. Danaei, M. R. M. M.; Dehghankhold, M.; Ataei, S.; Hasanzadeh Davarani, F.; Javanmard, R.; Dokhani, A.; Khorasani, S.; Mozafari, M. R. *Pharmaceutics* **2018**, *10*, 57.
- 15. Beltrán, J. J.; Barrero, C. A.; Punnoose, A. *Phys. Chem. Chem. Phys.* **2019**, *21*, 8808–8819.
- 16. Capanema, N. S. V.; Mansur, A. A. P.; Carvalho, I. C.; Carvalho, S. M.; Mansur, H. S. *Gels* **2023**, *9*, 166.



- 17. Zhang, F.; Dou, J.; Zhang, H. Polymers 2018, 10, 1340.
- 18. Wang, D.; Yang, J.; Xue, F.; Wang, J.; Hu, W. *Colloids Surf. A* **2021**, *612*, 126009.
- 19. Pomalaza, G.; Simon, P.; Addad, A.; Capron, M.; Dumeignil, F. *Green Chem.* **2020**, *22*, 2558–2574.
- Bian, T.; Gardin, A.; Gemen, J.; Houben, L.; Perego, C.; Lee, B.; Elad, N.; Chu, Z.; Pavan, G. M.; Klajn, R. *Nat. Chem.* 2021, *13*, 940–949.
- 21. Shevchenko, E. V.; Talapin, D. V.; Kotov, N. A.; O'Brien, S.; Murray, C. B. *Nature* **2006**, *439*, 55–59.
- 22. Levin, M. D.; Kaphan, D. M.; Hong, C. M.; Bergman, R. G.; Raymond, K. N.; Toste, F. D. *J. Am. Chem. Soc.* **2016**, *138*, 9682–9693.
- 23. Scaeteanu, G. V.; Maxim, C.; Badea, M.; Olar, R. *Molecules* **2023**, 28, 1132.